Preparation and Characterization of Polyelectrolyte-Coated Gold Nanoparticles

Annie Dorris, Simona Rucareanu, Linda Reven,* Christopher J. Barrett, and
R. Bruce Lennox

*Centre for Self-Assembled Chemical Structures (CSACS), Department of Chemistry, McGill University,
801 Sherbrooke Street West, Montreal, Quebec, Canada H3A 2K6*

Gold nanoparticles of 5 nm diameter, stabilized by 4-(dimethylamino)pyridine (DMAP), were coated with poly-(sodium 4-styrene sulfonate) (PSS) via electrostatic self-assembly. The suspension stability, monitored by the gold surface plasmon band (SPB), was studied by varying the pH, the PSS chain length, and PSS concentration. Enhanced stability is obtained at pH 10 (above the pK_a of DMAP) when the polymer chain length matches or exceeds the particle circumference. Solid state ^{13}C NMR was used to determine the presence of DMAP and polymers after subsequent deposition of weak and strong polycations: poly(allylamine hydrochloride) (PAH) and poly(diallyldimethylammonium chloride) (PDADMAC). At pH 10, DMAP remains associated with the nanoparticle after the first PSS layer has been formed. When PAH or PDADMAC are subsequently added at pH 4.5, DMAP is expelled, the suspensions remain stable, and zeta potential values indicate complete charge reversal. In the case of PDADMAC, however, the first layer of PSS is not fully retained. When PDADMAC is added at pH 10, DMAP and the first PSS layer are retained but lower zeta potentials and a higher SPB shift indicate a degraded stability. For PAH addition at pH 9.5, both DMAP and PSS are expelled and the suspension becomes unstable. These differences in stability of the multilayer components and the nanoparticle suspension are rationalized in terms of chain flexibility, polymer charge density, and the ability of the polymer functional groups to directly interact with the gold surface.

1. Introduction

The adsorption of polyelectrolyte multilayers onto oppositely charged colloidal particles using the layer-by-layer technique has been widely investigated experimentally,[1–4] and to a lesser extent theoretically.[5,6] The most studied experimental variables of polyelectrolyte assembly are the chain length and charge density, both of which affect the polymer chain flexibility, as well as the ionic strength of the solution medium and the substrate charge density. Electrophoresis, dynamic light scattering, transmission electron microscopy, and atomic force microscopy have also been employed to study the encapsulation of colloidal particles. Despite the considerable effort that has been made to understand this encapsulation process, many aspects remain unclear. A major obstacle is the ability to directly probe polymer/polymer and polymer/substrate interactions at the molecular level. However, recent solid-state NMR studies of polyelectrolyte multilayers have provided valuable insight into the chain dynamics, conformation, and the properties of the bound water, with layer number.[7–9]

Until now, attention has been focused mainly on polyelectrolyte multilayers deposited on flat substrates and micrometer-sized particles. In many applied fields, however, nanoparticles are the desired substrate. Such particles offer the advantage of a large surface area to volume ratio, offering a greater potential for catalysis[10] and drug delivery, both of which require a large surface of reactivity. Nanoparticles (NPs) also are of practical use for fundamental studies by techniques such as NMR spectroscopy, which requires high surface areas for sensitivity reasons. The disadvantage of nanoparticles lies in the possibility that the high surface curvature may restrict polymer adsorption due to limited chain flexibility. Consequently, poor polymer coverage can decrease the stability of colloidal suspensions required for many applications, especially with the smallest size particles.

Gold NPs are the most commonly used substrate for studying the polymer deposition onto a high-curvature surface. Gold NPs offer control of particle size and surface functionalities and can be stabilized by either weakly or strongly attached ligands. Caruso and co-workers[1,2,11] compared the encapsulation of gold NPs stabilized by both types of ligands. They concluded that the surface charge created by weak anions is insufficient to successfully adsorb polyelectrolytes onto highly curved surfaces, and the polyelectrolytes detach to form bulk polyampholyte complexes. On the other hand, highly charged NPs stabilized by covalently attached ligands were successfully encapsulated. However, Schneider and Decher[4] successfully deposited poly-electrolyte multilayers onto 12 nm diameter gold NPs stabilized by the labile citrate ions. Unlike Caruso, they claimed that ions on a gold surface are displaced by the incoming polyelectrolyte rather than associating with it. Since no direct investigations have been made to test this assumption, it is not clear what type of dynamics exists between the ligand and the polyelectrolyte at the particle surface and whether ions are truly displaced. Given that some of the most interesting recent applications of gold nanoparticles focus on the smallest (2–6 nm) particles, further study is obviously necessary, preferably through a full layering study.

* To whom correspondence should be addressed. E-mail: linda.reven@mcgill.ca.

(1) Gittins, D. I.; Caruso, F. *Adv. Mater.* **2000**, *12*, 1947.
(2) Gittins, D. I.; Caruso, F. *J. Phys. Chem. B* **2001**, *105*, 6846.
(3) Liang, Z.; Susha, A.; Caruso, F. *Chem. Mater.* **2003**, *15*, 3176.
(4) Schneider, G.; Decher, G. *Nano Lett.* **2004**, *4*, 1833.
(5) Chodanowski, P.; Stoll, S. *J. Chem. Phys.* **2001**, *115*, 4951.
(6) Haronska, P.; Vilgis, T. A.; Grottenmüller, R.; Schmidt, M. *Macromol. Theory Simul.* **1998**, *7*, 241.
(7) Smith, R. N.; Reven, L.; Barrett, C. J. *Macromolecules* **2003**, *36*, 1876.
(8) Smith, R. N.; McCormick, M.; Barrett, C. J.; Reven, L.; Spiess, H. W. *Macromolecules* **2004**, *37*, 4830.
(9) McCormick, M.; Smith, R. N.; Graf, R.; Barrett, C. J.; Reven, L.; Spiess, H. W. *Macromolecules* **2003**, *36*, 3616.

(10) Yu, A.; Liang, Z.; Cho, J.; Caruso, F. *Nano Lett.* **2003**, *3*, 1203.
(11) Mayya, K. S.; Schoeler, B.; Caruso, F. *Adv. Funct. Mater.* **2003**, *13*, 183.

In this paper, we systematically investigate the conditions required to deposit polyelectrolytes onto nanoparticles via electrostatic self-assembly. The system consists of 4−6 nm diameter gold NPs, stabilized by 4-dimethylaminopyridine (DMAP), a labile ligand, in an aqueous medium. DMAP stabilizes the gold NPs via a resonance form that involves an anion interacting with the Au surface. The result is a pyridine−Au interaction and a cationic ammonium being created which induces a positive charge at the gold surface.[12] Previous studies have reported successful incorporation of such particles into polyelectrolyte multilayers,[3,10,13−15] while others have demonstrated positive interactions between polyelectrolytes and Au−DMAP.[16−18] This current paper explores the encapsulation of Au−DMAP nanoparticles by poly(styrene sodium sulfonate) (PSS) and the possibility of adding subsequent polyelectrolyte layers. The influence of DMAP and polymer concentration and the polymer chain length on particle stability is investigated to optimize the suspension stability. The surface plasmon absorption of gold, transmission electron microscopy, and zeta potential measurements are used to assess the stability. Finally, the association of DMAP and PSS as well as the influence of subsequent layers is examined by solid-state NMR.

2. Experimental Section

2.1. Materials. Hydrogen tetrachloroaurate trihydrate (HauCl$_4$·3H$_2$O, 99.9999%) was purchased from Strem Chemicals. Tetra-octylammonium bromide (TOAB, 98%), sodium borohydride (NaBH$_4$, 99%), and 4-(*N,N*-dimethylaminopyridine (DMAP, 99%) were received from Aldrich. Poly(styrenesulfonic acid sodium salt) of molecular weight (Mw) 1400, 4300, 13000, 17000, 32000, and 49000, poly(allylamine hydrochloride) with a Mw of 15000, and poly(diallyldimethylammonium chloride) of Mw 15000 (measured by SLS) were purchased from Sigma. Au−DMAP nanoparticles (1 mg(Au)/mL) were synthesized using the Gittens and Caruso method.[12] Pure water of high resistivity (18.2 MΩ) was used for all sample preparation and was obtained by using a Milli-Q water system (Millipore Corporation).

2.2. Sample Preparation. Twenty-five milliliters of a 2 mg/mL PSS, 1 mM NaCl solution was added to 5 mL of 1 mg(Au)/mL Au−DMAP suspension. The optimum polymer concentration was determined by varying the PSS:DMAP$_{bound}$ ratio and the optimum adsorption was obtained for a 80:1 ratio. The mixture was sonicated for 20 min and left to stand another 40 min to allow for maximal adsorption. The solution was centrifuged at 21000 rpm for 1 h. Twenty milliliters of supernatant was removed and replaced by 20 mL of fresh water to rinse excess unadsorbed DMAP and polyelectrolyte. Eight centrifugation steps were performed in the stability study whereas five centrifugation steps were sufficient for NMR sample preparation. Subsequent layer depositions were performed based on the same adsorption procedure using PDADMAC and PAH solution of 2 mg/mL. In the case where pH adjustments were required, 1.0 M NaOH and 1% acetic acid solution were used.

Because considerable loss of sample occurs during centrifugation due to the small size of the particles (only 30% of particles recovered after five centrifugations), it is difficult to prepare a sufficient amount of sample for solid-state NMR that requires relatively large quantities. Forty milliliters of Au−DMAP suspensions was found to be sufficient to produce enough material for ^{13}C experiments (about 13 mg of coated Au−DMAP NPs). Samples were dried in a vaccum oven at room temperature for several hours and rehydrated with D$_2$O.

2.3. Surface Plasmon Band Measurements. The stability state of nanoparticle suspensions was monitored by UV−vis spectroscopy on a Cary 500 UV−visible spectrophotometer using 1 cm quartz cuvettes. Suspensions (see above) of 0.17 mg/mL of Au NPs were analyzed without dilution. The absorbance recorded at every centrifugation step was done at constant volume to allow critical comparison between samples. However, concentration between samples may change due to particle loss during rinsing. The DMAP concentration was estimated from its adsorption band at 268 nm (calibration curve was established beforehand). Aliquots of 20−200 µL of samples were diluted to 3 mL of Milli-Q water for UV measurements.

2.4. Electrophoretic Mobility (EPM) Measurements. Zeta potentials (ξ-potential) of Au−DMAP and coated Au−DMAP were measured on a Zeta Plus zeta potential analyzer (Brookhaven Instrument Corporation, New York). Samples holding 1 mg/mL Au were used for analysis and an average over 10 measurements was calculated for each sample.

2.5. Particle Visualization. Transmission electron microscopy (TEM) experiments were performed on a Philips CM200 TEM using an acceleration voltage of 200 kV. The point-to-point and line resolutions of the microscope were respectively 0.24 and 0.17 nm.

2.6. NMR Measurements. 150 MHz ^{13}C spectra were recorded on a Bruker ASX 600 spectrometer. Rotors (2.5 mm) were filled with mixtures of samples and KBR and were spun at 15 kHz. A recycle delay of 2 s, and a contact time of 2 ms were used. Proton ^{1}H 90° pulse widths of 5 µs were applied and an average of 15000 scans was recorded. The two-dimensional double-quantum back-to-back (2D DQ BABA) experiment was performed at the shortest recoupling time of one rotor period and a total number of 16 scans were recorded.

3. Results and Discussion

3.1. Optimization of Particle Stability. *3.1.1. Effect of pH and Concentration on Au−DMAP NPs.* The conditions used to optimize the adsorption of the first layer of PSS onto Au−DMAP NPs were explored. PSS exhibits a constant negative charge above pH 2, making it suitable to interact with positively charged DMAP molecules localized at a gold surface (DMAP$_{bound}$). Although previous work reported a positive interaction between DMAP and PSS, this interaction is not definitively understood.[16] Several groups have suggested that DMAP desorbs upon PSS adsorption[10,15] but no direct evidence has been presented. The system under investigation is rather complex because the capping layer is weakly bound to gold and must be present in large excess to stabilize the gold NPs. Free excess DMAP (DMAP$_{soln}$) may interfere with the subsequent PSS deposition. Unlike citrate ions [4], it is not possible to remove DMAP$_{soln}$ prior to polymer adsorption without destabilizing the suspension and losing a significant quantity of NPs. Moreover, the stability is greatly influenced by the DMAP concentration and the solution pH. An understanding of the roles that these variables play during the polymer adsorption is crucial for achieving optimal polymer adsorption and particle stability. UV−vis spectroscopy was initially used to monitor the PSS layer deposition. Au−DMAP NPs, prior to polymer deposition, exhibit a strong absorption band at 517 nm. The surface plasmon band (SPB) position is affected by interparticle interactions and the dielectric properties of the environment (solvent, ligand shell) that changes upon polymer adsorption.[19]

The absorbance of the Au−DMAP NPs is red-shifted by 12 nm upon adsorption of PSS (Figure 1). A combination of the change in dielectric and the reduction of interparticle distances due to bridging can contribute to this shift. However, the suspension remains clear with no evidence of particle precipita-

(12) Gittins, D. I.; Caruso, F. *Angew. Chem.* **2001**, *40*, 3001.
(13) Dong, W.-F.; Sukhorukov, G. B.; Mohwald, H. *Phys. Chem. Chem. Phys.* **2003**, *5*, 3003.
(14) Turkenburg, D. H.; Antipov, A. A.; Thathagar, M. B.; Rothenberg, G.; Sukhorukov, G. B.; Eiser, E. *Phys. Chem. Chem. Phys.* **2005**, *7*, 2237.
(15) Gittins, D. I.; Susha, A. S.; Schoeler, B.; Caruso, F. *Adv. Mater.* **2002**, *14*, 508.
(16) Cho, J.; Caruso, F. *Chem. Mater.* **2005**, *17*, 4547.
(17) Gandubert, V. J.; Lennox, B. *Langmuir* **2005**, *21*, 6532.
(18) Gandubert, V. J.; Lennox, B. Submitted to *Can. J. Chem.*

(19) Underwood, S.; Mulvaney, P. *Langmuir* **1994**, *10*, 3427.
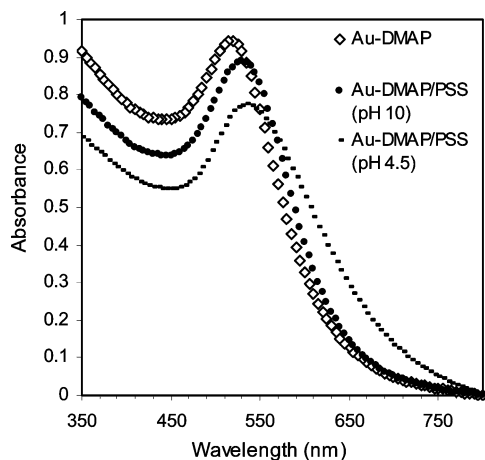
Figure 1. UV−vis spectrum of Au−DMAP and Au−DMAP coated with PSS at two different pHs.
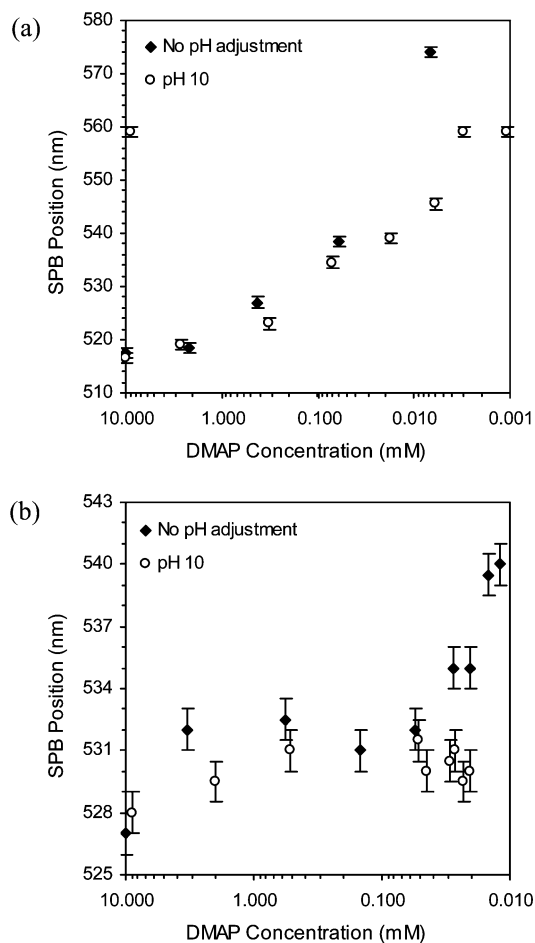

Figure 2. Evolution of the position of surface plasmon band of gold nanoparticles stabilized by (a) DMAP and (b) PSS at different pHs as DMAP is removed from the sample by centrifugation.

tion, suggesting a degree of stability. The particles coated with PSS at pH 4.5 exhibit a broad curve, reflecting particle aggregation. To examine in more detail the change in stability upon polymer coating while varying pH conditions, the position of the surface plasmon band was monitored after every centrifugation step (Figure 2). The DMAP concentration and pH of the solution gradually decrease with increasing the number of centrifugations. The pH and DMAP concentration variables are closely related since a decrease in DMAP concentration decreases the pH of the suspension. We recently reported that

the particle stability is limited to the pH range of 5−12 where the proportion of unprotonated DMAP is large enough to stabilize the particle.[17] Protonated DMAP is unable to bind to gold efficiently, leading to unprotected Au NPs that are highly susceptible to coalescence. The large pH range of stability relies on the fact that DMAP has two different pK_a values. $DMAP_{soln}$ has a pK_a of 9.6 and $DMAP_{bound}$ pK_a is around 5.[17] Surface plasmon band measurements of Au−DMAP NPs at a range of pH values demonstrate that the greatest stability is observed between pH 7.5 and 10 (SPB maximum 518−521 nm). Below pH 7.5, $DMAPH^+$ is the major form (99%) in solution and contributes less efficiently to maintaining great stability (SPB position >574 nm). Above pH 10, more than 70% neutral DMAP is present.

Prior to the layer deposition, changes in stability of the Au−DMAP NPs in different pH environments were explored for a better understanding of DMAP behavior (Figure 2a). Solution removal was then performed without pH adjustment and at a constant pH of 10 where DMAP is mostly unprotonated. After four centrifugations, the DMAP concentration was reduced to about 0.1 mM and the Au−NPs not submitted to any specific pH adjustment were no longer stable as reflected by the large SPB shift and the appearance of a blue film at the bottom of the sample. The pH at this stage is around 5; therefore, a great portion of the solution and adsorbed DMAP is protonated, making it unable to associate with gold and to be easily washed away during centrifugation. On the other hand, the suspensions maintained at pH 10 exhibit better stability even after seven centrifugations (DMAP ∼0.001 mM) is due to the fact that at this pH the DMAP is mostly unprotonated (86%), leading to strong association with gold. Moreover, the DMAP concentration has a less significant impact on particle stability, in agreement with Barlow and Burgess[20] who observed that DMAP coverage is only weakly dependent on the bulk surfactant concentration at high electrolyte pH. The presence of hydroxyl ions in solution at higher pH may also contribute to the stability of the Au−DMAP NPs through weak association with the DMAP bound layer, which may prevent its desorption.

Although the NPs remain in suspension, their stability is poor (SPB shift to 559 nm), establishing that the DMAP concentration still plays a role. The importance of excess DMAP on Au NPs stability is such that 1.6 mM DMAP is required to stabilize 1 mg/mL of nanoparticles, corresponding to a 2.5−3-fold excess of DMAP.[17] Therefore, the stability decrease observed after two centrifugations for both pH conditions (with and without pH adjustment) can be attributed to the reduction of free DMAP in solution to a level corresponding to 4% (about 0.4 mM) of the initial DMAP concentration (estimated by UV−vis measurements). It is however difficult to quantitatively assess the contribution of DMAP to stability since the nanoparticle concentration also decreases with the number of centrifugations.

3.1.2. Effect of pH and Concentration on Au−DMAP/PSS NPs. When PSS is added to the suspension (Figure 2b), a shift in the SPB is observed. However, good particle stability is maintained even after eight centrifugations, reflecting the effect of polymer adsorption. At this stage 0.1% DMAP (0.010 mM) is present in solution, showing that 30 times less DMAP (required concentration should be about 0.272 mM for a 0.17 mg/mL Au) is required to stabilize the original Au−DMAP NPs. The DMAP remaining in the suspension is expected to be associated with the PSS-coated Au NPs. To further confirm layer deposition, the zeta potential at the surface of the nanoparticle was measured.

(20) Barlow, B. C.; Burgess, I. J. *Langmuir* **2007**, *23*, 1555.

A potential alternation from +42 to −35 mV is obtained after polymer adsorption, consistent with a successful charge reversal.

The effect of pH on the particle coating was also investigated. In the case where no pH adjustment is performed, the stability decreases after four centrifugations. The pH at this stage is reduced, leading to DMAP desorption from the gold surface. In the case where the pH of the solution is maintained above 10 (above the $DMAP_{soln}$ pK_a) throughout the centrifugation process, the stability is not altered by the multiple centrifugations. $DMAP_{bound}$ clearly still plays a role in the particle stability, even after PSS is adsorbed.

3.1.3. Effect of the PSS Chain Length. The effect of polymer chain length was examined in the context of optimizing the encapsulation of the Au−DMAP NPs. Although computational simulations[5,6,21−25] were used to study the effect of the surface curvature on polymer adsorption, relatively few experimental investigations have been reported.[26] The stability depends greatly on the extent of adsorption and the conformation of the adsorbed polyelectrolyte,[5] which will be affected by a high surface curvature. Systematic studies of the variation of charge density,[25] stiffness,[23,27,28] and the chain length of a polyelectrolyte[5,21,24,25,28] demonstrate their effect on PE adsorption. In the present investigation, only the influence of the chain length was examined. The number of NaPSS segments varied from 7 to 240 and the ionic strength during the whole assembly process was restricted to the range of 2−5 mM, taking into account the contributions of $DMAPH^+$ and added NaCl. Although polymer adsorption is favored and charge reversal is increased with increasing ionic strength, it has been stated that to overcome the entropy loss per monomer due to adsorption, low ionic strengths are needed for shorter chain lengths.[21] Moreover, the introduction of an anionic species such as Cl^- and oxyanions[29] that can compete with DMAP adsorption is not desirable. However, under low ionic conditions, the flexibility of NaPSS is sacrificed since the polymer exhibits a more extended structure with a persistence length of about 6 nm,[30] which may in turn restrict the adsorption.[5,21]

The effect of chain length can be expressed either in terms of α_L (the ratio of the polymer chain length to the particle diameter) or in terms of R_g/R (the ratio of the radius of gyration of the polymer over the radius of the particle). In this study, we have chosen to express the chain length effect in terms of R_g/R. The radius of gyration of NaPSS was calculated using the Odijk approximation for the wormlike chain model and the ratio R_g/R can be estimated from the average particle radius that is about 5 nm. The suspension stability of the NPs was monitored via the position of the gold surface plasmon band. Figure 3 shows the SPB positions of gold−DMAP NPs coated with six different molecular weights of PSS.

These results show that the particle stability of a fresh as-prepared solution decreases when R_g/R < 1. Large red shifts consistent with NPs aggregation are observed. A blue deposit in the sample that accumulates with time also reflects poor stability. At small R_g/R values, theoretical studies assert that short polymer chains can fully spread on the surface.[21] The capacity to form contacts with the NPs surface is limited due to high monomer−
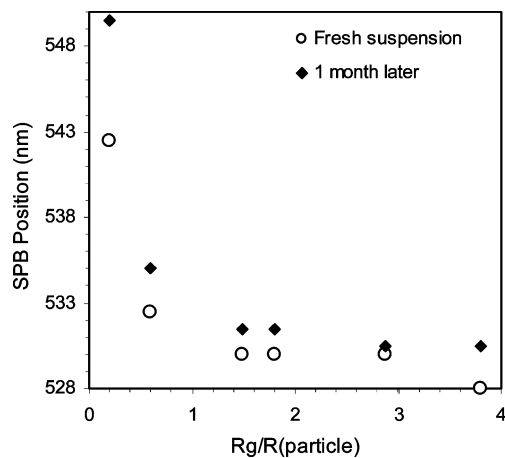

Figure 3. Stability change of particles coated with different polymer chain lengths with time.

monomer repulsion, causing weak charge inversion. Poor stabilities and zeta potentials of −10 mV, below the maximal charge inversion for NaPSS of −42 mV, confirm these assumptions. At $R_g/R \geq 1$, the particles maintain greater stability with time and exhibit a zeta potential of −41 mV, close to the maximal PSS charge reversal. This agrees with theoretical simulations that predict a more efficient wrapping of the polyelectrolyte around the particles that maximizes charge reversal when the particle size is of the order or greater than the radius of gyration of the polyelectrolyte.[5] TEM imaging confirms good particle stability for Au−DMAP coated with PSS having a R_g comparable to the particle radius as no visible aggregation is observed (Figure 4, right image); the nanoparticle size is conserved upon polyelectrolyte layer addition. For PSS with a R_g smaller than the particle radius, the TEM image (Figure 4, middle) demonstrates the limited capacity of short polymer chains to create a barrier to prevent aggregation. Caruso and co-workers also observed the successful encapsulation of 7 nm particles when using a polymer chain length which matches the particle circumference.[1,2] However, no systematic chain length study has been carried out. Because good stability is sought here, a medium PSS molecular weight of 17000 ($R_g/R \sim 1.8$) was used for the subsequent studies instead of the higher Mw PSS (Mw 49000; $R_g/R \sim 3.8$) to avoid flocculation via chain bridging between particles.

3.2. NMR Characterization of the Au/DMAP/PSS Interactions. Solid-state ^{13}C CP MAS NMR spectroscopy was used to verify whether $DMAP_{bound}$ still plays a role in NPs stabilization after PSS encapsulation. To prevent DMAP desorption from gold that reduces particle stability, the pH during the coating process was maintained at 10, well above the $DMAP_{bound}$ pK_a. Figure 5a presents the ^{13}C CP MAS NMR spectra of solid PSS/DMAP mixture in a 1:1 ratio that was produced by precipitation from aqueous solution. Mixtures prepared at different pHs showed no effect on the chemical shifts. The peaks at 40, 107, 150, and 155 ppm correspond to DMAP while the peaks at 40, 126, and 142−152 ppm are from the PSS. Overlapping between DMAP and PSS occurs in the aromatic region and near 40 ppm; however, the 107 ppm peak of DMAP is well-resolved. Proton spin lattice relaxation measurements revealed different T_1 values for DMAP and PSS. The lack of a common proton T_1 indicates the presence of a physical mixture rather than a closely associated complex. The sharp peaks of the DMAP are characteristic of a crystalline material whereas the resonances of PSS, an amorphous polymer, are relatively broad.

The ^{13}C NMR spectrum of PSS coated on Au−DMAP NPs is shown in Figure 5b. We observe peaks similar to the ones

(21) Chodanowski, P.; Stoll, S. *Macromolecules* **2001**, *34*, 2320.
(22) Kong, C. J.; Muthukumar, M. *J. Chem. Phys.* **1998**, *109*, 1522.
(23) Stoll, S.; Chodanowski, P. *Macromolecules* **2002**, *35*, 9556.
(24) Netz, R. R.; Joanny, J.-F. *Macromolecules* **1999**, *32*, 9026.
(25) Jonsson, M.; Linse, P. *J. Chem. Phys.* **2001**, *115*, 3406.
(26) McQuigg, D. W.; Kaplan, J. I.; Dubin, P. L. *J. Phys. Chem.* **1992**, *96*, 1973.
(27) Wallin, T.; Linse, P. *Langmuir* **1996**, *12*, 305.
(28) Akinchina, A.; Linse, P. *Macromolecules* **2002**, *35*, 5183.
(29) Cumberland, S. L.; Strouse, G. F. *Langmuir* **2002**, *18*, 269.
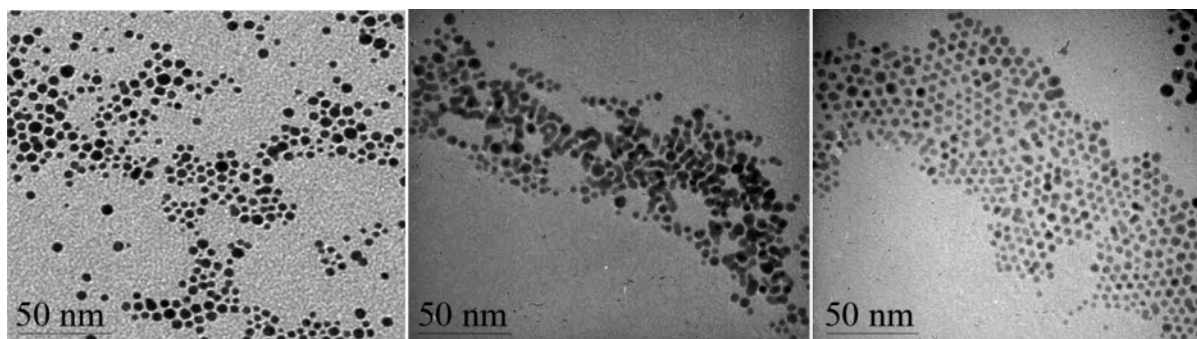(30) Spiteri, M. N.; Boué, F.; Lapp, A.; Cotton, J. P. *Phys. Rev. Lett.* **1996**, *77*, 5218.

Figure 4. TEM images of Au−DMAP (left), Au−DMAP/PSS with $R_g/R = 0.1$ (middle), and Au−DMAP/PSS with $R_g/R = 1.8$ (right). The scale bar is 50 nm.
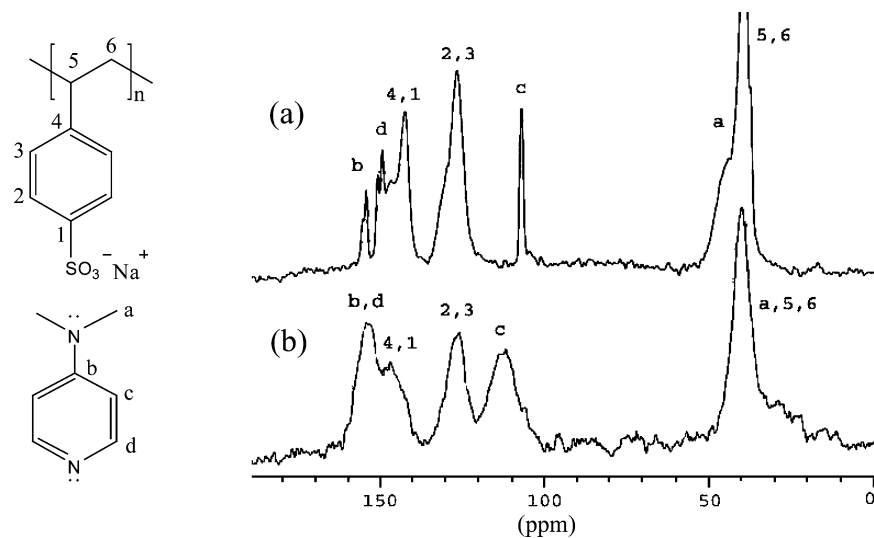

Figure 5. ^{13}C CP MAS spectra of (a) DMAP/PSS solid mixture and (b) Au−DMAP/PSS.

observed in the bulk-state PSS/DMAP, confirming the presence of DMAP in the system. However, the overall broadening and some changes in the chemical shifts of the DMAP resonances reflect its interaction with the gold nanoparticle surface. The distinct aromatic signal at 112 ppm DMAP is shifted downfield as compared to that of bulk DMAP ($\delta = 107$ ppm). Although DMAP presence is observed, no direct evidence of electrostatic interactions between the capping agent and the polyelectrolyte is confirmed.

In an attempt to directly detect complexation between PSS and the DMAP$_{bound}$, a two-dimensional ^{1}H double quantum (DQ) MAS NMR experiment was performed. Proton−proton proximities less than 3.5 Å can be detected by the appearance of a double quantum signal. Prior to the 2D ^{1}H DQ MAS NMR experiment, a single quantum ^{1}H MAS NMR spectrum was collected to distinguish the peak corresponding to associated water and to confirm its suppression in the double quantum experiment.[31]

Figure 6 presents a ^{1}H DQ MAS NMR spectrum of Au−DMAP coated with PSS. Autocorrelation peaks of PSS and DMAP$_{bound}$ are observed around 7 and 15 ppm in the double quantum dimension (F1 axis) corresponding to the aliphatic and aromatic signals. The extensive overlapping of proton spectra of PSS and DMAP hinders identification of cross-peaks that would identify close spatial proximity of the DMAP$_{bound}$ and PSS protons. Weak and unresolved cross-correlation peaks appear around 10 ppm in the F1 axis. These peaks correspond to the sum
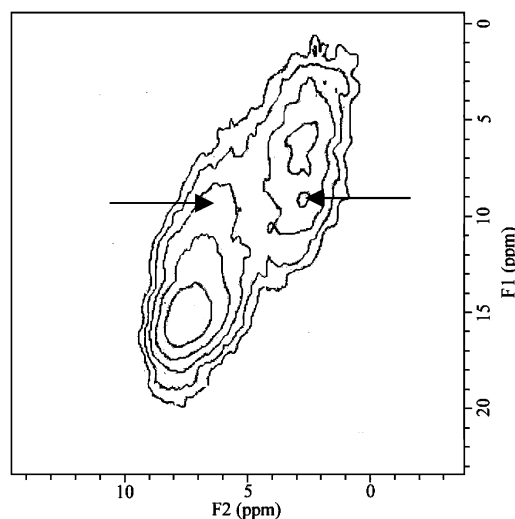
(31) Rodriguez, L. N. J.; De Paul, S. M.; Barrett, C. J.; Reven, L.; Spiess, H. W. *Adv. Mater.* **2000**, *12*, 1934.

Figure 6. 2D DQ BABA of Au−DMAP/PSS recorded at a rotor spinning frequency of 25 kHz. F1 axis represents the double quantum dimension whereas F2 axis represents the single quantum dimension. Arrows indicate the positions of weak cross-correlation peaks.

of the chemical shift of protons that undergo DQ resonances and may correspond to a combination of aromatic proton from PSS and DMAP$_{bound}$ and methyl protons of DMAP. NOESY type experiments of samples saturated with D$_2$O to increase the mobility and the resolution may allow detection of the DMAP−PSS association.
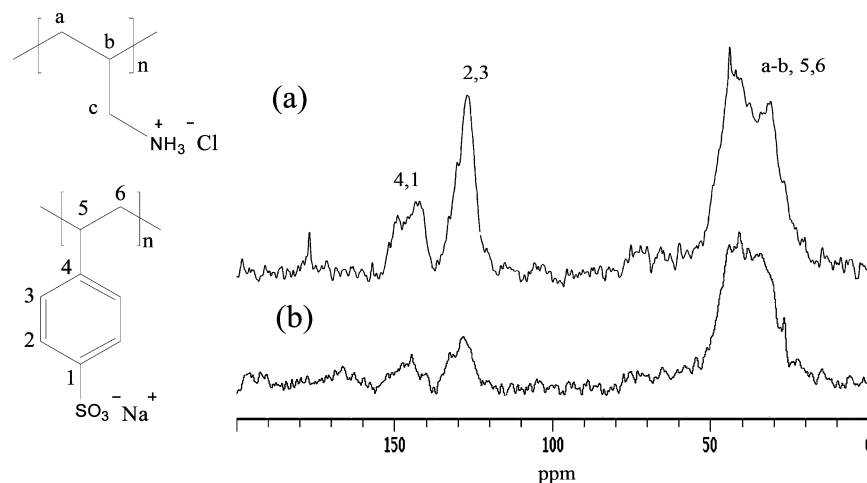
Figure 7. [13]C of Au−DMAP/PSS/PAH with polycation assembled at (a) pH 4.5 and (b) pH 9.5.

Table 1. Summary of Surface Plasmon Band (SPB) Position, Zeta Potential, and Solids NMR Characterization of PSS/Au−DMAP NPs Coated with Weak (PAH) or Strong (PDADMAC) Polycations

polycation (second layer)	pH	SPB position (nm)	zeta potential (mV)	DMAP	PSS	interactions
PAH	4.5	533	+41	absent	fully retained	strong PSS−PAH complexation; DMAP released by pH effect
	9.5	553	+44	absent	reduced	weak PSS−PAH compexation; DMAP released by PAH displacement
PDADMAC	4.5	533	+45	absent	reduced	PSS−PDADMAC complexation; DMAP released by pH effect
	10	535	+25	partially retained	fully retained	PSS−PDADMAC complexation; high pH favors Au−DMAP interaction

3.3. Influence of Subsequent Layer Deposition. Two different polycations were deposited on the first PSS layer: PDADMAC, a strong polyelectrolyte, and PAH, a weak polyelectrolyte (pK_a of 8.6). The SPB shifts, zeta potential, and NMR results are summarized in Table 1. Successful layer deposition is confirmed by charge reversal and the SPB shift. The deposition of a second layer of polymer was performed at two different pH values (near pH 4.5 where complete DMAP desorption is expected and between pH 9−10). The pH of the PAH solution is restricted to 9.5 since above this pH the reduced net charge of PAH induces particle bridging. The addition of a subsequent layer does not change the SPB position significantly when PDADMAC and PAH (at pH 4.5) are assembled on the NPs. However, a drastic SPB shift is observed when PAH is assembled at pH 9.5. At this pH, only about 12% of the amino groups on the PAH backbone are charged, reducing the electrostatic repulsion between particles. The zeta potentials are fairly large and positive, providing evidence of polymer deposition. However, to understand the actual role of PSS and DMAP$_{bound}$ and to predict whether the polymer substitution or association takes place during the polycation deposition, direct spectroscopic observation of the components at the NPs surface is required.

Figure 7 presents the ^{13}C spectrum of PAH assembled on Au−DMAP/PSS NPs at pH 4.5 and 9.5. At low pH, well-defined aromatic PSS peaks appear between 126 and 146 ppm whereas overlapping PAH and PSS peaks are observed at 33 and 40 ppm, respectively. The capping agent DMAP is absent from the spectra, which can be explained by the pH effect that induces DMAPH$^+$ release. The preserved association between the bilayer and the metal, originally provided by DMAP$_{bound}$ might then possibly be attributed to the benzyl sulfonate group of PSS. Sulfonate oxyanions d-orbitals are capable of relieving excess charges at the metal surface through back-bonding, which confers to the ligand−metal interaction a partial covalent character that in turn enhances the interaction strength.[29] Cyclic voltametry on the adsorption of benzylsulfonate anions on a Au(111) single-crystal electrode demonstrate a rather strong interaction between the

metal and the ligand.[32] Figure 7b presents the ^{13}C spectrum of PAH assembled at pH 9.5 that shows clear evidence of bilayer disruption: PSS peak intensities are significantly reduced and DMAP is absent from the spectrum. At this pH condition, the unprotonated form of PAH dominates (89%), making amino groups available for binding to gold. Although the binding of amino groups with gold is known to be relatively weak,[33] stabilization of gold NPs via the NH$_2$ group in the main chain of chitosan has been successfully employed by several groups.[34−37] Increased flexibility due to reduced repulsion on the polymer backbone in combination with a weaker association with PSS can explain the partial PSS removal and DMAP displacement. Unlike the fully protonated PAH, the mostly neutral polymer can reorganize within the multilayer to reach the NPs surface and displace both DMAP and a significant amount of PSS. Furthermore, the fact that PSS is partially displaced from gold reveals a stronger affinity of the primary amine to gold. On the other hand, at pH 9.5 the adsorbed PAH is only weakly charged and the NPs consequently exhibit poor suspension stability as indicated by the shift of the SPR to 553 nm.

The ^{13}C CP MAS NMR spectra of a PDADMAC−PSS bilayer coated at two different pHs are presented in Figure 8. The PDADMAC characteristic peaks are observed at 71, 55, and 27 ppm. Unresolved peaks are also present in the region between 30 and 40 ppm where PSS and PDADMAC peaks overlap. In Figure 8a, no DMAP is detected and PSS peaks intensities are reduced relative to the intensities expected for a 1:1 ratio.[7] As seen with the PAH deposition, DMAP bonding to gold is not favored at this pH. In contrast to PAH, PDADMAC seems to

(32) Dutkiewicz, E.; Skotuda, P. *J. Chem. Soc., Faraday Trans.* **1996**, *92*, 3767.
(33) McCleverty, J. A., Meyer, T. J., Eds. *Comprehensive Coordination Chemistry II*; Elsevier: Oxford, UK, 2004; Vol. 6.
(34) Huang, H.; Yang, X. *Biomacromolecules* **2004**, *5*, 2340.
(35) Dos Santos, D. S.; Goulet, P. J. G.; Pieczonka, N. P. *Langmuir* **2004**, *20*, 5918.
(36) Miyama, T.; Yonezawa, Y. *Langmuir* **2004**, *20*, 5918.
(37) Karadas, F.; Ertas, G.; Ozkaraoglu, E.; Suzer, S. *Langmuir* **2005**, *21*, 437.
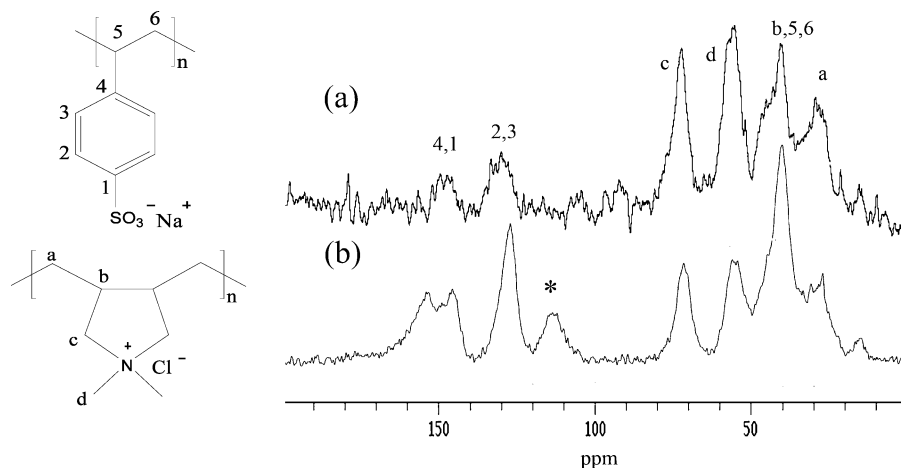
Figure 8. ^{13}C CP MAS NMR spectra of Au−DMAP/PSS/PDADMAC with polycation assembled at (a) pH 4.5 and (b) pH 10. ∗ indicates the presence of DMAP.

displace a significant amount of PSS. The nanoparticle stabilization can then occur through the formation of ion pairs via the chlorine PDADMAC counterion that specifically associates with the gold surface. This has already been observed in the preparation of gold clusters using a quaternary ammonium bromide salt as the phase-transfer agent[38] and more recently in the stabilization of NPs by *N,N,N*-trimethylchitosan chloride.[39] The variation between PDADMAC and PAH deposition possibly comes from a difference in stiffness and complexation strength. Despite the fact that PAH carries a Cl^- that can weakly associate with gold, its inability to reorganize, once complexed with PSS due to strong ion-pairing interactions,[40] can prevent the $NH_3^+Cl^-$ group from competing with the $R-SO_3^-$ group for gold surface sites. On the other hand, the relatively flexible PDADMAC exhibits stronger interactions toward its Cl^- counterion and consequently forms weaker complexes with PSS. This major difference in stiffness and electrostatic attraction toward PSS can explain the inability of PAH to displace PSS as compared to PDADMAC.

When PDADMAC is added to the Au−DMAP/PSS NPs at pH 10 (Figure 8b), DMAP is still present in the spectrum and the PSS peaks remain intense. At this pH, PSS remains strongly bound to the surface via the DMAP and can preserve its positive electrostatic association to PDADMAC without being displaced by the polycation.

(38) Fink, J.; Kiely, C. J.; Bethell, D.; Schiffrin, D. J. *Chem. Mater.* **1998**, *10*, 922.

(39) Ding, Y.; Xia, X.-H.; Zhang, C. *Nanotechnology* **2006**, *17*, 4156.

(40) Jaber, J. A.; Schlenoff, J. B. *Langmuir* **2007**, *23*, 896.

Conclusion

Under selected assembly conditions consisting of a pH maintained above the $DMAP_{soln}$ pK_a and a polymer radius of gyration comparable to the particle radius, DMAP-stabilized gold NPs can be encapsulated by PSS to yield extremely stable suspensions. Solid-state NMR spectroscopy provides valuable insight into the polymer and DMAP/gold surface interactions as the assembly pH and type of polyion are varied. There is an electrostatic association between $DMAP_{bound}$ and PSS, rather than a ligand substitution by the incoming polyelectrolyte. When a subsequent layer composed of a weak or a strong polycation is added, the stability of the bilayer is dictated by the nature of the multiple, weak interactions of the polymer functional groups (SO_3, NH_2, $N(CH_3)_2^+Cl^-$, $NH_3^+Cl^-$) with the gold surface relative to that of $DMAP_{bound}$, which in turn is influenced by the assembly pH. Future work will focus on the influence of these surface interactions and the high surface curvature on the properties and stability of polyelectrolyte multilayers deposited on nanoparticles.